



Quantum correlations of light and matter through environmental transitions

Iles-Smith, Jake; Nazir, Ahsan

Published in:
Optica

Link to article, DOI:
[10.1364/OPTICA.3.000207](https://doi.org/10.1364/OPTICA.3.000207)

Publication date:
2016

Document Version
Publisher's PDF, also known as Version of record

[Link back to DTU Orbit](#)

Citation (APA):
Iles-Smith, J., & Nazir, A. (2016). Quantum correlations of light and matter through environmental transitions. *Optica*, 3(2), 207-211. <https://doi.org/10.1364/OPTICA.3.000207>

General rights

Copyright and moral rights for the publications made accessible in the public portal are retained by the authors and/or other copyright owners and it is a condition of accessing publications that users recognise and abide by the legal requirements associated with these rights.

- Users may download and print one copy of any publication from the public portal for the purpose of private study or research.
- You may not further distribute the material or use it for any profit-making activity or commercial gain
- You may freely distribute the URL identifying the publication in the public portal

If you believe that this document breaches copyright please contact us providing details, and we will remove access to the work immediately and investigate your claim.

Quantum correlations of light and matter through environmental transitions

Jake Iles-Smith^{1,2,3,*} and Ahsan Nazir^{1,3,†}

¹*Photon Science Institute & School of Physics and Astronomy,*

The University of Manchester, Oxford Road, Manchester M13 9PL, United Kingdom

²*Department of Photonics Engineering, DTU Fotonik, Ørstedsgade, 2800 Kongens Lyngby, Denmark*

³*Controlled Quantum Dynamics Theory, Imperial College London, London SW7 2AZ, United Kingdom*

(Dated: April 1, 2016)

One aspect of solid-state photonic devices that distinguishes them from their atomic counterparts is the unavoidable interaction between system excitations and lattice vibrations of the host material. This coupling may lead to surprising departures in emission properties between solid-state and atomic systems. Here we predict a striking and important example of such an effect. We show that in solid-state cavity quantum electrodynamics, interactions with the host vibrational environment can generate quantum cavity-emitter correlations in regimes that are semiclassical for atomic systems. This behaviour, which can be probed experimentally through the cavity emission properties, heralds a failure of the semiclassical approach in the solid-state, and challenges the notion that coupling to a thermal bath supports a more classical description of the system. Furthermore, it does not rely on the spectral details of the host environment under consideration and is robust to changes in temperature. It should thus be of relevance to a wide variety of photonic devices.

INTRODUCTION

The diversity of systems studied in cavity quantum electrodynamics (CQED) places the subject at the heart of many prospective quantum and classical technologies. Examples include single photon sources [1, 2], ultrafast optical switches [3, 4], and quantum gates [5–7], which require the development of robust, scalable, and potentially strongly coupled emitter-cavity systems. Though the quantum strong coupling (QSC) limit and beyond—in which the system eigenstates become light-matter entangled—have now been attained for single emitters in the microwave regime [8, 9], it remains technically demanding to manufacture optical cavities of sufficiently high quality (Q) factor to unambiguously demonstrate QSC phenomena. Example systems in which great strides have recently been made towards this goal include single self-assembled quantum dots (QDs) within optical nano- and microcavities [10–14]. Here, small mode volumes can readily be obtained, resulting in potentially large Q-factors and cavity coupling strengths that are substantial in comparison to the emitter decay rate. In conjunction with their solid state nature, this makes QD-cavity systems excellent candidates for future technological applications.

Nevertheless, it still remains a challenging endeavour to reach the QSC regime due to significant cavity losses [15, 16]. The broad cavity lineshape that results masks contributions from higher order dressed states. This places the system in an intermediate coupling regime that can be described using semiclassical techniques [17], thus neglecting all quantum correlations between the cavity photonic (light) and emitter electronic (matter) degrees of freedom. In addition to interactions with external electromagnetic fields, many CQED systems are also in contact with their host (e.g. thermal)

environment; for example, in QDs this influence is often dominated by acoustic phonons [18, 19]. In order to explore the effect that such couplings have on the system's optical emission, it is necessary to modify the standard quantum optical treatments [20], which may lead to significant departures from atomic-like behaviour [21–30].

Here, we demonstrate that quantum light-matter correlations can be generated in solid-state CQED systems via transitions induced by the host (vibrational) environment, in regimes of semiclassical atomic CQED emission where such an environment is absent. Specifically, we show that the presence of the host environment results in optical emission that is observably sensitive to the joint eigenstructure of the cavity and emitter, even when the equivalent atomic transitions are not, and quantify the resulting deviations from the semiclassical description. This behaviour, which may be probed experimentally through asymmetries in both the cavity reflectivity and emission spectra, also challenges the notion that the addition of a thermal environment should simply decohere our system to a more classical effective description. We stress that the quantum correlations we shall describe, though mediated by the solid-state environment, are shared between the light and matter degrees of freedom of the CQED system itself (i.e. cavity photons and internal emitter electronic states) and *not* with the host environment.

MODEL

We consider a driven cavity coupled to a single two level emitter (TLE), shown schematically in Fig. 1(a). This is a model of wide importance, though later we shall consider specific parameters relevant to QD-microcavity systems to provide experimental context [10, 12, 16, 31–

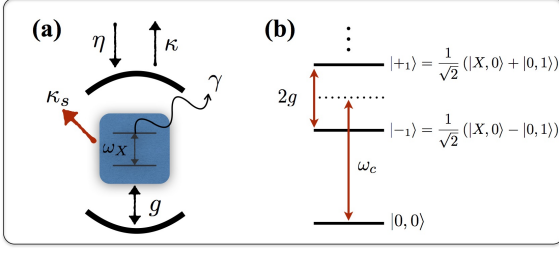


FIG. 1. (a) Schematic of the emitter-cavity setup considered. The cavity is one sided, driven by a continuous-wave laser of frequency ω_L with strength η , and loses excitation through the top (sides) with rate κ (κ_s). The TLE decay rate is γ , and the TLE-cavity coupling strength is g . (b) The first rung of the dressed state ladder, i.e. the lowest eigenstates of the coupled TLE-cavity system, in the absence of dissipation and driving.

33]. Within a frame rotating at the laser frequency ω_L , and after a rotating-wave approximation, the system Hamiltonian is

$$H_S = \delta \sigma^\dagger \sigma + g (\sigma^\dagger a + \sigma a^\dagger) + \eta (a^\dagger + a) + \mu a^\dagger a. \quad (1)$$

Here, $\mu = \omega_C - \omega_L$ and $\delta = \omega_X - \omega_L$ are, respectively, the cavity-laser and emitter-laser detunings, g is the emitter-cavity interaction strength, η is the cavity-laser coupling, $\sigma = |0\rangle\langle X|$ is the lowering operator for the TLE, and a is the annihilation operator for the cavity mode.

To highlight the qualitative changes in behaviour brought about in the solid-state by the presence of the host environment, we formulate a rigorous model of its impact on the system through a polaron representation master equation [22, 24–26, 30]. This can then be related to the cavity optical emission through the input-output formalism [34]. Here we consider the environment to be described by a collection of harmonic oscillators, with free Hamiltonian $H_B = \sum_k \nu_k b_k^\dagger b_k$, where b_k^\dagger (b_k) is the creation (annihilation) operator for mode k . The TLE-environment interaction is given by $H_I = \sigma^\dagger \sigma \sum_k f_k (b_k^\dagger + b_k)$, and its effect on the system may be described by the spectral density, which we take to have a super-Ohmic form appropriate to acoustic phonon processes, $J(\nu) = \sum_k f_k^2 \delta(\nu - \nu_k) = \alpha \nu^3 e^{-\nu^2/\Lambda^2}$, with α the coupling strength and Λ a high frequency cut-off [18, 19].

Applying the polaron transformation, $\mathcal{U} = \exp\{-\sigma^\dagger \sigma \sum_k f_k (b_k^\dagger - b_k)/\nu_k\}$, to the full Hamiltonian $H = H_S + H_B + H_I$ allows us to derive a master equation valid beyond the weak TLE-environment coupling regime [35]. This unitary generates a displaced representation of the thermal bath, removing the linear coupling term H_I to give

$$\tilde{H} = \mathcal{U}^\dagger H \mathcal{U} = \delta \sigma^\dagger \sigma + g B (\sigma^\dagger a + \sigma a^\dagger) + \eta (a^\dagger + a) + \mu a^\dagger a + (X B_X + Y B_Y) + \sum_k \nu_k b_k^\dagger b_k, \quad (2)$$

where we have absorbed the polaron shift to the emitter frequency, $\Delta_{\text{pol}} = \sum_k f_k^2/\nu_k$, into the definition of ω_X . Here, the TLE-cavity coupling strength has been renormalised by the average displacement of the oscillator environment, $g \rightarrow gB$, with $B = \text{tr}(B_\pm \rho_{\text{th}})$ denoting the expectation of the displacement operators $B_\pm = \exp\{\pm \sum_k f_k (b_k^\dagger - b_k)/\nu_k\}$ with respect to the thermal state $\rho_{\text{th}} = \exp\{-\beta \sum_k \nu_k b_k^\dagger b_k\}/\text{tr}(\exp\{-\beta \sum_k \nu_k b_k^\dagger b_k\})$ at inverse temperature $\beta = 1/k_B T$. The transformed operators are $X = g(\sigma^\dagger a + \sigma a^\dagger)$, $Y = ig(\sigma^\dagger a - \sigma a^\dagger)$, $B_X = (1/2)(B_+ + B_- - 2B)$, and $B_Y = (i/2)(B_+ - B_-)$.

Moving into the interaction picture with respect to the coupled TLE-cavity Hamiltonian in the polaron frame, $\tilde{H}_S = \delta \sigma^\dagger \sigma + gB (\sigma^\dagger a + \sigma a^\dagger) + \eta(a^\dagger + a) + \mu a^\dagger a$, we derive a master equation for their reduced state, $\rho(t)$, by tracing out the environment within a second-order Born-Markov approximation. In essence, this procedure may be thought of as a perturbative expansion about the parameter g/Λ [25], and is thus non-perturbative in the TLE-environment coupling strength, capturing multi-phonon processes [36]. Nevertheless, as the renormalised coupling term $gB (\sigma^\dagger a + \sigma a^\dagger)$ appears explicitly in the system Hamiltonian \tilde{H}_S , this expansion does not preclude the exploration of TLE-cavity dressed states.

Including photon emission from both the TLE and cavity, within a Born-Markov approximation and assuming the radiation field outside the cavity to have a flat spectrum [20, 37, 38], our master equation takes the Schrödinger picture form [25, 39]:

$$\dot{\rho}(t) = -i[\tilde{H}_S, \rho(t)] + \mathcal{K}_{\text{th}}[\rho(t)] + \frac{\gamma}{2} \mathcal{L}_\sigma[\rho(t)] + \frac{\kappa + \kappa_s}{2} \mathcal{L}_a[\rho(t)]. \quad (3)$$

Here, $\mathcal{L}_x[\rho] = 2x\rho x^\dagger - \{x^\dagger x, \rho\}$, γ is the TLE spontaneous emission rate, and κ (κ_s) is the photon loss rate from the top (sides) of the cavity. The superoperator $\mathcal{K}_{\text{th}}[\rho(t)] = -([X, \Phi_X \rho(t)] + [Y, \Phi_Y \rho(t)] + \text{H.c.})$, with $\Phi_X = B^2 \int_0^\infty (e^{\varphi(\tau)} + e^{-\varphi(\tau)} - 1) e^{-i\tilde{H}_S \tau} X e^{i\tilde{H}_S \tau} d\tau$, $\Phi_Y = B^2 \int_0^\infty (e^{\varphi(\tau)} - e^{-\varphi(\tau)}) e^{-i\tilde{H}_S \tau} Y e^{i\tilde{H}_S \tau} d\tau$, and $\varphi(\tau) = \int_0^\infty \nu^{-2} J(\nu) (\coth(\beta\nu/2) \cos \nu\tau - i \sin \nu\tau) d\nu$, accounts for interactions with the thermal bath as just described. When referring to the standard quantum optical master equation (QOME) used to describe atomic systems, phonon processes are absent such that the Hamiltonian in Eq. (3) reduces to that given in Eq. (1), i.e. $\tilde{H}_S \rightarrow H_S$, while $\mathcal{K}_{\text{th}}[\rho(t)] \rightarrow 0$.

To relate the internal emitter-cavity degrees of freedom described by Eq. (3) directly to observable experimental signatures, we note that in most CQED setups it is not the system expectation values that are directly probed, but rather the emitted cavity photons. For example, we can obtain cavity reflectivity spectra from Eq. (3) by way of the input-output formalism [34], which draws a formal connection between system operators and those of

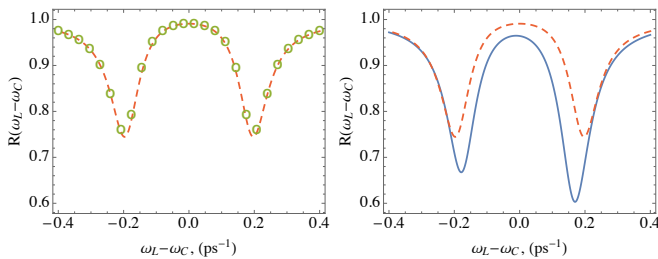


FIG. 2. Steady-state reflectivity in the intermediate coupling regime, showing (left) agreement between the semiclassical theory (points) and the atomic QOME (dashed), and (right) deviations from the atomic QOME (dashed) once the solid-state environment is included (solid). We choose parameters relevant to QD-microcavity setups [10, 12, 16, 31–33]: $\kappa = g = 0.2 \text{ ps}^{-1}$, $\eta = 0.001 \text{ ps}^{-1}$, $\kappa_s = 0.025 \text{ ps}^{-1}$, $\gamma^{-1} = 300 \text{ ps}$, $\alpha = 0.075 \text{ ps}^2$, $\Lambda = 2.2 \text{ ps}^{-1}$, and $T = 4 \text{ K}$.

the cavity emitted field. Heisenberg-Langevin equations are first used to define collective field operators for both the input, \hat{a}_{in} , and output, \hat{a}_{out} through the top of the cavity, leading to the famous input-output relation [34]: $\hat{a}_{out}(t) - \hat{a}_{in}(t) = \sqrt{\kappa}\hat{a}(t)$. It is then straightforward to derive an expression for the complex cavity reflectivity in the steady state: $r = \langle \hat{a}_{out} \rangle / \langle \hat{a}_{in} \rangle = 1 - i(\kappa/\eta)\langle \hat{a} \rangle$, where $R = |r|$ gives the reflectivity coefficient.

RESULTS

Having outlined our theoretical approach, let us focus our analysis on what we shall term the intermediate coupling regime, as it has particular experimental relevance to optical microcavities [15, 16] (we analyse the classical Fano and QSC limits in the Supplementary Material). Here, $\kappa + \kappa_s \gtrsim g > \gamma$, such that cavity leakage is significant. For an atomic system, this regime is characterised by a symmetric double dip structure in the steady state reflectivity spectrum on scanning a weak driving field through resonance. This can be seen by the dashed curve in Fig. 2 (left) which treats the TLE-cavity coupling fully quantum mechanically through the QOME. The dips lie at resonances of the first two eigenstates of the TLE-cavity system, that is, the first rung of the dressed state ladder [see Fig. 1(b)]. However, unlike the true QSC regime (in which $g > \kappa + \kappa_s, \gamma$), the broad cavity transition obscures contributions from higher order dressed states, allowing an effective semiclassical description to be derived [16, 17]. The double dip structure may then be interpreted simply as a normal mode splitting between two classical oscillators, rather than a signature of quantum light-matter correlations. This can be shown in the atomic case by considering the relevant optical Bloch equations, obtained from the QOME: $\langle \dot{\sigma} \rangle = -(i\mu + \frac{\gamma}{2})\langle \sigma \rangle + ig\langle \sigma_z a \rangle$, $\langle \dot{a} \rangle = -(i\mu + \frac{\kappa + \kappa_s}{2})\langle a \rangle - ig\langle \sigma \rangle - i\eta$, with $\langle \hat{O} \rangle = \text{tr}(\hat{O}\rho)$. Applying a mean-field approximation between the cavity

and TLE, such that $\langle \sigma_z a \rangle \approx \langle \sigma_z \rangle \langle a \rangle$, neglects any quantum correlations accumulated between them, i.e. they remain in a product state. In the weak driving limit, we may further assume that on average the TLE remains close to its ground state, such that $\langle \sigma_z \rangle \approx -1$ [17, 40]. For a sufficiently lossy cavity, the resulting semiclassical theory agrees perfectly with the atomic QOME, as is demonstrated by the points in Fig. 2 (left).

Discrepancies in the cavity reflectivity become apparent, however, when comparing to the full (polaron) master equation relevant to solid-state CQED. We now see a shift in the dip positions due to bath renormalisation of the TLE-cavity coupling, and an asymmetry in the cavity reflectivity that was entirely absent in either the QOME or semiclassical calculations. Importantly, this implies that the semiclassical description breaks down here even within a weakly-driven and lossy cavity regime, as we shall quantify below, and thus the addition of a thermal environment *generates quantum correlations* within our system. In the Supplementary Material we also show that these features cannot be reproduced by a phenomenological pure-dephasing description of the host environment, and that differences persist between the atomic and solid-state cases even at stronger driving.

In fact, we can attribute these asymmetric features to the quantum mechanical nature of the host environment, which plays a vital role in determining the system dynamics. In Fig. 2, where we have chosen parameters relevant to the acoustic phonon environment common in QD-microcavity systems, bath-induced transitions occur on a faster timescale than other dissipative processes, i.e. cavity leakage and spontaneous emission. The phonon bath is thus sensitive to coherence shared between the cavity and QD emitter, with the result that it mediates transitions directly between the emitter-cavity dressed states. Specifically, when we tune the driving field to the upper dressed state resonance ($\omega_L - \omega_C \approx 0.2 \text{ ps}^{-1}$), phonon emission allows population to transfer from the upper to the lower dressed state, with an associated loss of energy to the environment. This leads to a suppression of the upper dressed state population and also of the reflected light. Provided that the temperature is not too high, the inverse process, which raises population from the lower to the upper dressed state by phonon absorption, is comparatively weaker. The resulting asymmetries herald a failure of the semiclassical theory, which by definition cannot be sensitive to the coherence shared between the TLE and cavity. This is a somewhat counterintuitive point. Naively, one might think of phonons purely as a source of decoherence, that is, as giving rise to processes that should push the system towards a more classical description. However, here we see that the sensitivity of the host environment to quantum correlations in fact results in the breakdown of the semiclassical description of our system, and we must instead reinstate a quantum mechanical explanation.

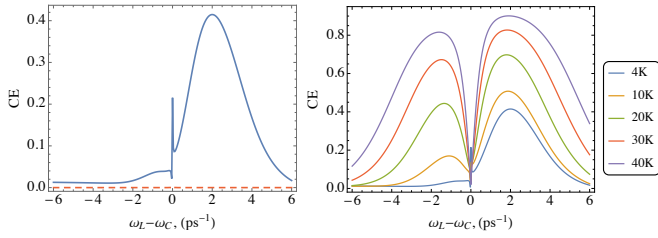


FIG. 3. Left: Correlation error as a function of detuning, comparing the atomic QOME (dashed) and solid-state polaron master equation (solid) at $T = 4$ K. Right: Correlation error at increasing temperature (lower to upper curves) for the solid-state master equation. All other parameters are as in Fig. 2.

Further quantitative insight into departures from the semiclassical theory can be gained by considering the correlation error (CE), defined in Ref. [41] as

$$\text{CE} = |\langle \sigma^\dagger a \rangle - \langle \sigma^\dagger \rangle \langle a \rangle| / |\langle \sigma^\dagger a \rangle|, \quad (4)$$

which is a measure of the quantum correlations shared between the cavity photons and TLE electronic states. Fig. 3 (left) shows the CE for both the QOME (dashed) and full polaron (solid) master equations at $T = 4$ K. Here, the QOME shows no observable accumulation of correlations over the full range of detunings, confirming that we are in a semiclassical regime of atomic emission. In contrast, within the solid-state theory significant correlations are apparent across a broad range of driving frequencies, induced by the action of the thermal environment. This unambiguously demonstrates the breakdown of the semiclassical description of our solid-state CQED system due to the presence of the host environment.

It is natural to ask whether the effects we predict are robust against variations in temperature. The asymmetries in the cavity lineshapes presented in Fig. 2 do indeed decrease as a function of increasing temperature due to environmental absorption processes balancing emission. However, from Fig. 3 (right) we see that the CE is enhanced substantially as a function of temperature for both positive and negative detuning, due to the associated increase in phonon emission and absorption rates. Thus the semiclassical theory remains insufficient to characterise the TLE-cavity system even as temperature is increased. Despite the fact that lineshape asymmetries decrease at high temperatures, deviations from the semiclassical theory can still be observed experimentally by looking at the spectra of photons emitted from the cavity when driving either the lower or upper dressed state resonantly. In the former case, only at very low temperatures should we expect emission centred solely around the lower dressed state, while in the latter, the same bath-mediated transitions that are responsible for correlations should lead to emission from both the lower and upper dressed states at all temperatures, in stark contrast to

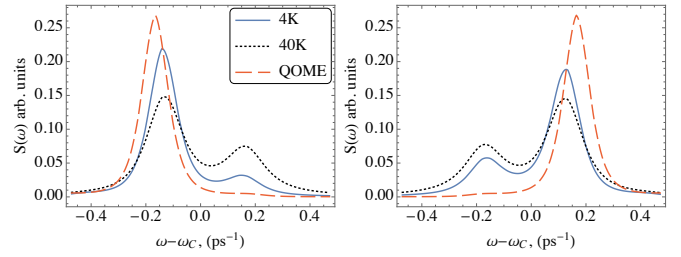


FIG. 4. Comparison of the cavity emission spectra using the atomic QOME (dashed) and solid-state polaron master equation (solid and dotted), under resonant excitation of the lower dressed state (left) and the upper dressed state (right) transitions. Parameters are as in Fig. 2, except $\eta = 0.05$ ps $^{-1}$.

the conventional atomic expectation.

In Fig. 4 we plot the cavity incoherent emission spectrum, $S(\omega) \propto \text{Re}[\int_0^\infty g_{inc}^{(1)}(\tau) e^{i(\omega_L - \omega)\tau} d\tau]$, with $g_{inc}^{(1)}(\tau) = \lim_{t \rightarrow \infty} \langle a^\dagger(t + \tau) a(t) \rangle - |\langle a^\dagger \rangle_{ss}|^2$ obtained from our master equations using the quantum regression theorem [20, 42]. Here $\langle a^\dagger \rangle_{ss}$ is the steady state expectation value of the cavity operator, which describes coherent emission. In the atomic case (dashed curves), Fig. 4 shows the expected resonant response from a normal mode, with a single dominant peak centred around whichever is the driven dressed state transition. However, the spectra are markedly different for the solid-state CQED system, where we see a suppression of the dominant peak and the emergence of an additional feature centred around the *opposite* dressed state to the one being driven. As anticipated, this is a consequence of transitions mediated by the host environment, which lead to the possibility of emission even around the undriven dressed state frequency. For lower temperatures (4 K), emission dominates, and the effect is thus more prominent in the right hand panel. However, at larger temperatures (40 K) absorption becomes almost as significant. Hence, by measuring the spectrum of light emitted from the cavity, we can unambiguously demonstrate the presence of bath-mediated transitions between the joint eigenstates of the emitter-cavity system (at both low and high temperatures), evidencing also the quantum mechanical nature of the host environment.

SUMMARY

In summary, we have shown that the presence of a thermal environment allows one to generate light-matter quantum correlations in solid-state CQED systems within otherwise semiclassical regimes. Sensitivity of the environment to the coherence shared between the TLE and cavity leads to direct transitions between their joint eigenstates, and consequently to a breakdown of the semiclassical approach. The resulting experimentally observable effects persist over a broad range of param-

ters, and should thus be applicable to a variety of CQED systems, such as QDs in micropillar and photonic crystal cavities [3, 10–16], diamond colour centres [43–45], and superconducting circuits [8, 9, 46], where fluctuating resistances in the host material may be mapped to an oscillator environment [47].

We thank D. P. S. McCutcheon, T. M. Stace, K. R. McEnery, R. Oulton, A. B. Young, and S. Carswell for discussions. J.I.-S. is supported by the Danish Research Councils, grant number DFF – 4181-00416 and A.N. by The University of Manchester through a Photon Science Institute Research Fellowship.

* jakeil@fotonik.dtu.dk

† ahsan.nazir@manchester.ac.uk

- [1] D. Press, S. Götzinger, S. Reitzenstein, C. Hofmann, A. Löffler, M. Kamp, A. Forchel, and Y. Yamamoto, “Photon antibunching from a single quantum-dot-microcavity system in the strong coupling regime,” *Phys. Rev. Lett.* **98**, 117402 (2007).
- [2] P. Michler, A. Kiraz, C. Becher, W. V. Schoenfeld, P. M. Petroff, L. Zhang, E. Hu, and A. Imamoglu, “A quantum dot single-photon turnstile device,” *Science* **290**, 2282–2285 (2000).
- [3] R. Bose, D. Sridharan, H. Kim, G. S. Solomon, and E. Waks, “Low-photon-number optical switching with a single quantum dot coupled to a photonic crystal cavity,” *Phys. Rev. Lett.* **108**, 227402 (2012).
- [4] V. Loo, C. Arnold, O. Gazzano, A. Lemaitre, I. Sagnes, O. Krebs, P. Voisin, P. Senellart, and L. Lanco, “Optical nonlinearity for few-photon pulses on a quantum dot-pillar cavity device,” *Phys. Rev. Lett.* **109**, 166806 (2012).
- [5] T. Pellizzari, S. Gardiner, J. Cirac, and P. Zoller, “Decoherence, continuous observation, and quantum computing: a cavity QED model,” *Phys. Rev. Lett.* **75**, 3788–3791 (1995).
- [6] L. M. Duan, M. D. Lukin, J. I. Cirac, and P. Zoller, “Long-distance quantum communication with atomic ensembles and linear optics,” *Nature* **414**, 413–418 (2001).
- [7] C.-H. Su, A. Greentree, W. Munro, K. Nemoto, and L. Hollenberg, “High-speed quantum gates with cavity quantum electrodynamics,” *Phys. Rev. A* **78**, 062336 (2008).
- [8] A. Wallraff, D. I. Schuster, A. Blais, L. Frunzio, R.-S. Huang, J. Majer, S. Kumar, S. M. Girvin, and R. J. Schoelkopf, “Strong coupling of a single photon to a superconducting qubit using circuit quantum electrodynamics,” *Nature* **431**, 162–167 (2004).
- [9] T. Niemczyk, F. Deppe, H. Huebl, E. P. Menzel, F. Hocke, M. J. Schwarz, J. J. Garcia-Ripoll, D. Zueco, T. Hümmer, E. Solano, A. Marx, and R. Gross, “Circuit quantum electrodynamics in the ultrastrong-coupling regime,” *Nature Phys.* **6**, 772 (2010).
- [10] J. P. Reithmaier, G. Sek, A. Löffler, C. Hofmann, S. Kuhn, S. Reitzenstein, L. V. Keldysh, V. D. Kulakovskii, T. L. Reinecke, and A. Forchel, “Strong coupling in a single quantum dot–semiconductor microcavity system,” *Nature* **432**, 197 (2004).
- [11] T. Yoshie, A. Scherer, J. Hendrickson, G. Khitrova, H. M. Gibbs, G. Rupper, C. Ell, O. B. Shchekin, and D. G. Deppe, “Vacuum Rabi splitting with a single quantum dot in a photonic crystal nanocavity,” *Nature* **432**, 200 (2004).
- [12] K. Hennessy, A. Badolato, M. Winger, D. Gerace, M. Atatüre, S. Gulde, S. Fält, E. L. Hu, and A. Imamoglu, “Quantum nature of a strongly coupled single quantum dot–cavity system,” *Nature* **445**, 896 (2007).
- [13] A. Faraon, I. Fushman, D. Englund, N. Stoltz, P. Petroff, and J. Vuckovic, “Coherent generation of non-classical light on a chip via photon-induced tunnelling and blockade,” *Nature Phys.* **4**, 859 (2008).
- [14] J. Kasprzak, S. Reitzenstein, E. A. Muljarov, C. Kistner, C. Schneider, M. Strauss, S. Höfling, A. Forchel, and W. Langbein, “Up on the jaynes–cummings ladder of a quantum-dot/microcavity system,” *Nature Mat.* **9**, 304 (2010).
- [15] C. Hu, A. Young, J. O’Brien, W. Munro, and J. Rarity, “Giant optical faraday rotation induced by a single-electron spin in a quantum dot: Applications to entangling remote spins via a single photon,” *Phys. Rev. B* **78**, 085307 (2008).
- [16] A. B. Young, R. Oulton, C. Y. Hu, A. C. T. Thijssen, C. Schneider, S. Reitzenstein, M. Kamp, S. Höfling, L. Worschech, A. Forchel, and J. G. Rarity, “Quantum-dot-induced phase shift in a pillar microcavity,” *Phys. Rev. A* **84**, 011803 (2011).
- [17] C. Y. Hu and J. G. Rarity, “Extended linear regime of cavity-qed enhanced optical circular birefringence induced by a charged quantum dot,” *Phys. Rev. B* **91**, 075304 (2015).
- [18] A. J. Ramsay, T. M. Godden, S. J. Boyle, E. M. Gauger, A. Nazir, B. W. Lovett, A. M. Fox, and M. S. Skolnick, “Phonon-induced Rabi-frequency renormalization of optically driven single InGaAs/GaAs quantum dots,” *Phys. Rev. Lett.* **105**, 177402 (2010).
- [19] A. J. Ramsay, A. V. Gopal, E. M. Gauger, A. Nazir, B. W. Lovett, A. M. Fox, and M. S. Skolnick, “Damping of exciton Rabi rotations by acoustic phonons in optically excited InGaAs/GaAs quantum dots,” *Phys. Rev. Lett.* **104**, 017402 (2010).
- [20] H. Carmichael, *Statistical Methods in Quantum Optics* (Springer, 1998).
- [21] D. P. S. McCutcheon and A. Nazir, “Coherent and incoherent dynamics in excitonic energy transfer: Correlated fluctuations and off-resonance effects,” *Phys. Rev. B* **83**, 165101 (2011).
- [22] D. P. S. McCutcheon and A. Nazir, “Quantum dot Rabi rotations beyond the weak exciton–phonon coupling regime,” *New J. Phys.* **12**, 113042 (2010).
- [23] Y.-J. Wei, Y. He, Y.-M. He, C.-Y. Lu, J.-W. Pan, C. Schneider, M. Kamp, S. Höfling, D. P. S. McCutcheon, and A. Nazir, “Temperature-dependent mollow triplet spectra from a single quantum dot: Rabi frequency renormalization and sideband linewidth insensitivity,” *Phys. Rev. Lett.* **113**, 097401 (2014).
- [24] C. Roy and S. Hughes, “Influence of electron–acoustic-phonon scattering on intensity power broadening in a coherently driven quantum-dot–cavity system,” *Phys. Rev. X* **1**, 021009 (2011).
- [25] D. P. S. McCutcheon and A. Nazir, “Model of the optical emission of a driven semiconductor quantum dot: Phonon-enhanced coherent scattering and off-resonant sideband narrowing,” *Phys. Rev. Lett.* **110**, 217401 (2013).

- [26] C. Roy and S. Hughes, “Phonon-dressed mollow triplet in the regime of cavity quantum electrodynamics: Excitation-induced dephasing and nonperturbative cavity feeding effects,” *Phys. Rev. Lett.* **106**, 247403 (2011).
- [27] S. Hughes and H. J. Carmichael, “Phonon-mediated population inversion in a semiconductor quantum-dot cavity system,” *New J. Phys.* **15**, 053039 (2013).
- [28] P. Kaer, P. Lodahl, A.-P. Jauho, and J. Mørk, “Microscopic theory of indistinguishable single-photon emission from a quantum dot coupled to a cavity: The role of non-Markovian phonon-induced decoherence,” *Phys. Rev. B* **87**, 081308 (2013).
- [29] P. Kaer and J. Mørk, “Decoherence in semiconductor cavity QED systems due to phonon couplings,” *Phys. Rev. B* **90**, 035312 (2014).
- [30] I. Wilson-Rae and A. Imamoglu, “Quantum dot cavity-QED in the presence of strong electron-phonon interactions,” *Phys. Rev. B* **65**, 235311 (2002).
- [31] M. Nomura, Y. Ota, N. Kumagai, S. Iwamoto, and Y. Arakawa, “Large vacuum Rabi splitting in single self-assembled quantum dot-nanocavity system,” *Applied Physics Express* **1**, 072102 (2008).
- [32] R. Ohta, Y. Ota, M. Nomura, N. Kumagai, S. Ishida, S. Iwamoto, and Y. Arakawa, “Strong coupling between a photonic crystal nanobeam cavity and a single quantum dot,” *Applied Physics Letters* **98**, 173104 (2011).
- [33] E. Peter, P. Senellart, D. Martrou, A. Lemaître, J. Hours, J. M. Gérard, and J. Bloch, “Exciton-photon strong-coupling regime for a single quantum dot embedded in a microcavity,” *Phys. Rev. Lett.* **95**, 067401 (2005).
- [34] M. J. Collett and C. W. Gardiner, “Squeezing of intracavity and traveling-wave light fields produced in parametric amplification,” *Phys. Rev. A* **30**, 1386–1391 (1984).
- [35] D. P. S. McCutcheon, N. S. Dattani, E. M. Gauger, B. W. Lovett, and A. Nazir, “A general approach to quantum dynamics using a variational master equation: Application to phonon-damped Rabi rotations in quantum dots,” *Phys. Rev. B* **84**, 081305(R) (2011).
- [36] A. Würger, “Strong-coupling theory for the spin-phonon model,” *Phys. Rev. B* **57**, 347 (1998).
- [37] K. Roy-Choudhury and S. Hughes, “Theory of phonon-modified quantum dot photoluminescence intensity in structured photonic reservoirs,” *Opt. Lett.* **40**, 1838–1841 (2015).
- [38] K. Roy-Choudhury and S. Hughes, “Spontaneous emission from a quantum dot in a structured photonic reservoir: phonon-mediated breakdown of fermi’s golden rule,” *Optica* **2**, 434–437 (2015).
- [39] M. Scala, B. Militello, A. Messina, J. Piilo, and S. Maniscalco, “Microscopic derivation of the Jaynes-Cummings model with cavity losses,” *Phys. Rev. A* **75**, 013811 (2007).
- [40] E. Waks and D. Sridharan, “Cavity QED treatment of interactions between a metal nanoparticle and a dipole emitter,” *Phys. Rev. A* **82**, 043845 (2010).
- [41] S. Hughes and C. Roy, “Nonlinear photon transport in a semiconductor waveguide-cavity system containing a single quantum dot: Anharmonic cavity-QED regime,” *Phys. Rev. B* **85**, 035315 (2012).
- [42] D. P. McCutcheon, “Optical signatures of non-Markovian behaviour in open quantum systems,” arXiv:1504.05970 (2015).
- [43] A. Faraon, C. Santori, Z. Huang, V. M. Acosta, and R. G. Beausoleil, “Coupling of nitrogen-vacancy centers to photonic crystal cavities in monocrystalline diamond,” *Phys. Rev. Lett.* **109**, 033604 (2012).
- [44] J. Riedrich-Möller, L. Kipfstuhl, C. Hepp, E. Neu, C. Pauly, F. Mücklich, A. Baur, M. Wandt, S. Wolff, M. Fischer, S. Gsell, M. Schreck, and C. Becher, “One- and two-dimensional photonic crystal microcavities in single crystal diamond,” *Nature Nanotech.* **7**, 69 (2012).
- [45] R. Albrecht, A. Bommer, C. Deutsch, J. Reichel, and C. Becher, “Coupling of a single nitrogen-vacancy center in diamond to a fiber-based microcavity,” *Phys. Rev. Lett.* **110**, 243602 (2013).
- [46] L. S. Bishop, J. M. Chow, J. Koch, A. A. Houck, M. H. Devoret, E. Thuneberg, S. M. Girvin, and R. J. Schoelkopf, “Nonlinear response of the vacuum Rabi resonance,” *Nature Phys.* **5**, 105–109 (2009).
- [47] M. H. Devoret, *Quantum Fluctuations in Electrical Circuits, Les Houches, Session LXIII* (Elsevier Science, 1997).

SUPPLEMENTAL MATERIAL

Here we give details on several aspects of solid-state cavity quantum electrodynamics (CQED) systems supplementary to the main text. We first highlight that a pure dephasing approximation is insufficient to capture host environment induced asymmetries (and more generally environmental processes) in solid-state photonic devices. We then discuss the role of driving strength in altering the cavity reflectivity spectra and comparisons between the semiclassical, atomic, and solid-state cases. Finally, we consider the influence of a thermal environment in the Fano and quantum strong coupling regimes of CQED, both of which are important to a variety of physical implementations.

Pure dephasing noise

A phenomenological approach to modelling noise processes in solid-state systems can be obtained by assuming a pure dephasing form for the dissipator, that is, the master equation

$$\begin{aligned} \frac{\partial \rho(t)}{\partial t} = & -i[H_s, \rho(t)] + \frac{\gamma}{2}\mathcal{L}_\sigma[\rho(t)] + \frac{\kappa}{2}\mathcal{L}_a[\rho(t)] \\ & + \frac{\Gamma}{2}\mathcal{L}_{\sigma_z}[\rho(t)], \end{aligned} \quad (5)$$

where the final term represents pure dephasing with rate Γ , and replaces the full environmental superoperator used in the main manuscript. Here, $\mathcal{L}_x[\rho(t)] = 2x\rho x^\dagger - \{x^\dagger x, \rho\}$ denotes a non-unitary dissipator in Lindblad form, while the system Hamiltonian, H_s , and the other rates are exactly as defined in the main manuscript.

Despite its use in the literature, the pure dephasing master equation is insufficient to fully capture noise processes in solid-state photonic systems [1]. One of the primary reasons for this is its disregard for the inter-

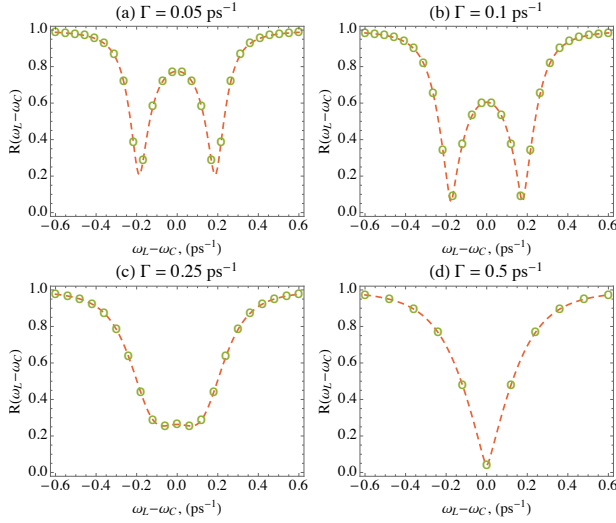


FIG. 5. Effects of pure dephasing on the cavity reflectivity spectra predicted by the pure dephasing master equation of Eq. 5 (dashed) and the semiclassical theory (points). Other parameters: $\kappa = g = 0.2 \text{ ps}^{-1}$, $\kappa_s = 0.025 \text{ ps}^{-1}$, $\gamma^{-1} = 300 \text{ ps}$.

nal eigenstructure of the system under consideration, which as shown in the manuscript is essential to accurately model processes induced by the host environment. For example, in Fig. 5 we consider an emitter-cavity system in the same parameter regime as Fig. 2 of the main manuscript. We see that increasing the pure dephasing rate leads to a symmetric broadening of the cavity reflectivity spectra, with the semiclassical theory (now including pure dephasing) remaining valid over the full range of dephasing rates. Such a phenomenological treatment cannot, therefore, lead to the deviations from semiclassicality that we predict with a full microscopic treatment of the solid-state environment.

Driving dependence and cavity asymmetry

The semiclassical equations derived in the main manuscript rely on the assumption of small emitter occupations, that is, $\langle \sigma_z \rangle \approx -1$. This is valid at weak driving, when the emitter remains close to its ground state, rarely scattering a photon. It stands to reason then that at strong driving, the semiclassical expressions derived previously will become invalid. For example, they are unable to capture driving dependent broadening of the cavity emission [2].

Despite this eventual failure, the semiclassical theory remains a robust description of the atomic (though of course not the solid-state) cavity reflectivity even when the driving strength increases by an order of magnitude from that considered in the main manuscript ($\eta = 0.001 \text{ ps}^{-1}$), as demonstrated in Fig. 6 (a) and (b). As

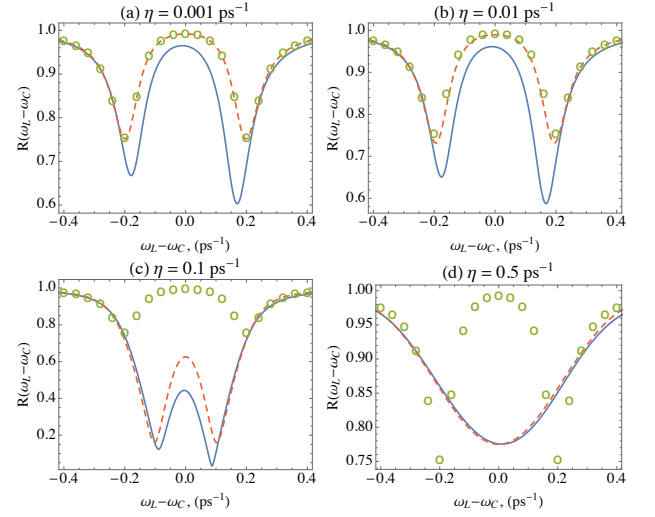


FIG. 6. Cavity reflectivity for increasing driving strength derived from the atomic QOME (dashed), semiclassical theory (points), and the solid-state polaron master equation (solid). Other parameters: $\kappa = g = 0.2 \text{ ps}^{-1}$, $\kappa_s = 0.025 \text{ ps}^{-1}$, $\gamma^{-1} = 300 \text{ ps}$, $\alpha = 0.075 \text{ ps}^2$, $\Lambda = 2.2 \text{ ps}^{-1}$, and $T = 4 \text{ K}$.

the driving strength increases yet further, the line shape broadens until the normal mode splitting is no longer visible, leaving only a single peak in the cavity reflectivity spectra as shown in Fig. 6 (d) at extremely strong driving. Nevertheless, signatures of phonon processes can remain observable outside the semiclassical limit, with asymmetries present even when the driving is of the same order as the cavity loss and light-matter coupling strength, see Fig. 6 (c).

The Fano and quantum strong coupling regimes

The sensitivity of the solid-state CQED system optical properties to the host environment is not restricted to the intermediate coupling regime described in the main manuscript. In fact, we shall demonstrate that similar effects emerge in the both the Fano and the quantum strong coupling (QSC) regimes.

The Fano regime of cavity QED occurs when $\kappa + \kappa_s \gg g \gg \gamma$, where κ and κ_s are the cavity loss and side-leakage rates respectively. This regime is characterised by a sharp peak in the cavity reflectivity at the emitter resonance (while the rest of the cavity line shape remains unchanged), which is the result of classical interference between two competing decay pathways [3]. This behaviour can be seen in line shapes given in Fig. 7 (a) and (b). Here we see excellent agreement between the semiclassical theory and the atomic QOME, showing a sharp peak in the reflectivity spectra at the emitter resonance $\Delta = \pm 0.5 \text{ ps}^{-1}$, which is symmetric for both the positively and negatively detuned cases. Though less pronounced than in the intermediate coupling regime,

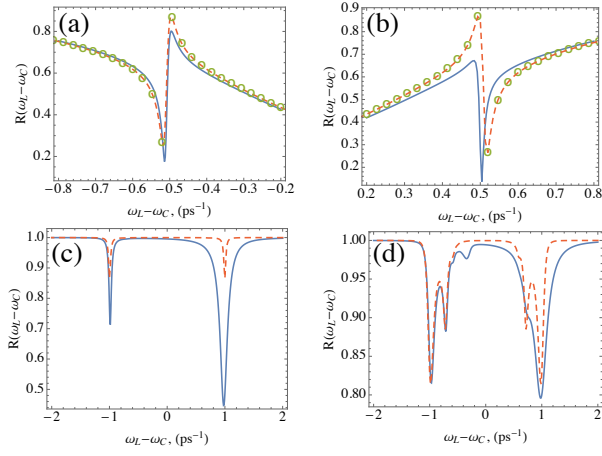


FIG. 7. Upper: Asymmetry in Fano resonance profiles between emitter-cavity detuning $\omega_C - \omega_X = -0.5 \text{ ps}^{-1}$ (a), and $\omega_C - \omega_X = 0.5 \text{ ps}^{-1}$ (b). Parameters are $\eta = 0.003 \text{ ps}^{-1}$, $\kappa = 1 \text{ ps}^{-1}$, $g = 0.1 \text{ ps}^{-1}$, $\kappa_s = 0.5 \text{ ps}^{-1}$, $\gamma^{-1} = 300 \text{ ps}$, $\Lambda = 2.2 \text{ ps}^{-1}$, $\alpha = 0.1 \text{ ps}^{-1}$, and $T = 2 \text{ K}$. Lower: Thermal effects in the QSC regime at weak driving $\eta = 0.005 \text{ ps}^{-1}$ (c), and strong driving $\eta = 0.08 \text{ ps}^{-1}$ (d). Parameters are $\kappa = 0.1 \text{ ps}^{-1}$, $g = 1 \text{ ps}^{-1}$, $\kappa_s = 0$, $\gamma^{-1} = 300 \text{ ps}$, $\Lambda = 2.2 \text{ ps}^{-1}$, $\alpha = 0.025 \text{ ps}^{-1}$, and $T = 4 \text{ K}$. Here points correspond to the semiclassical theory, dashed curves to the atomic QOME, and solid curves to the solid-state polaron theory.

host environment induced asymmetries become apparent when comparing the cavity line shape obtained from the full polaron master equation for an emitter tuned above the cavity resonance ($\omega_C - \omega_X = 0.5$) and below ($\omega_C - \omega_X = -0.5$).

In the QSC limit [Fig. 7 (c) and (d)], the coupling strength g becomes the dominant energy scale, $g \gg \kappa + \kappa_s, \gamma$, which allows contributions from higher order dressed states to be resolved. Additionally, the long cavity lifetime results in host environmental influences becoming particularly significant. This is especially true at strong driving, shown in Fig. 7 (d), where in the polaron theory the asymmetric broadening is so pronounced that it prevents us from resolving any higher order contributions to the upper dressed state resonance.

* jakeil@fotonik.dtu.dk

† ahsan.nazir@manchester.ac.uk

- [1] A. Nazir and D. P. S. McCutcheon, J. Phys.: Condens. Matter **28**, 103002 (2016).
- [2] C. Y. Hu and J. G. Rarity, Phys. Rev. B **91**, 075304 (2015).
- [3] A. E. Miroshnichenko, S. Flach, and Y. S. Kivshar, Rev. Mod. Phys. **82**, 2257 (2010).